PHYSICAL REVIEW C **79**, 061601(R) (2009)

Reaction cross sections at intermediate energies and Fermi-motion effect

M. Takechi,[1,*] M. Fukuda,[1] M. Mihara,[1] K. Tanaka,[2] T. Chinda,[1] T. Matsumasa,[1] M. Nishimoto,[1] R. Matsumiya,[1] Y. Nakashima,[1] H. Matsubara,[1] K. Matsuta,[1] T. Minamisono,[3] T. Ohtsubo,[4] T. Izumikawa,[5] S. Momota,[6] T. Suzuki,[7] T. Yamaguchi,[7] R. Koyama,[4] W. Shinozaki,[4] M. Takahashi,[4] A. Takizawa,[4] T. Matsuyama,[4] S. Nakajima,[7] K. Kobayashi,[7] M. Hosoi,[7] T. Suda,[2] M. Sasaki,[8] S. Sato,[9] M. Kanazawa,[9] and A. Kitagawa[9]

[1]*Department of Physics, Osaka University, Osaka 560-0043, Japan*
[2]*RIKEN, Nishina Center, Wako, Saitama 351-0198, Japan*
[3]*Fukui University of Technology, Fukui 910-8505, Japan*
[4]*Department of Physics, Niigata University, Niigata 950-2102, Japan*
[5]*RI Center, Niigata University, Niigata 951-8510, Japan*
[6]*Kochi University of Technology, Kami, Kochi 782-8502, Japan*
[7]*Department of Physics, Saitama University, Saitama 338-3570, Japan*
[8]*Ritsumeikan University, Shiga 525-8577, Japan*
[9]*National Institute of Radiological Sciences, Chiba 263-8555, Japan*

(Received 2 August 2008; revised manuscript received 14 March 2009; published 1 June 2009)

Precise measurements of the reaction cross sections (σ_R) for ^{12}C on Be, C, and Al targets and ^{11}Be on Be targets were performed in the energy range between 30 and 400 MeV/nucleon. The energy dependencies of σ_R for ^{12}C, ^{11}Be, and ^{8}B were compared to Glauber-type calculations performed using reliable nucleon-density distributions that are supported by experimental data. It was found that the Glauber-type calculations, which include the higher-order multiple scattering effect, the finite-range effect, and the Fermi-motion effect of nucleons in the nucleus, seem to provide a good prescription relating σ_R at intermediate energies to a proper nucleon-density distribution. This method provides a powerful tool with which to study the nuclear surface structure through the σ_R measurements.

DOI: 10.1103/PhysRevC.79.061601 PACS number(s): 25.60.Dz, 21.10.Gv, 24.10.−i

The nucleus-nucleus reaction cross section (σ_R) has played a crucial role in the studies of halo and skin structures in nuclei far from the line of stability [1]. A number of nuclear radii have been deduced from interaction cross sections ($\sigma_I \simeq \sigma_R$) measured at high energies (∼1 GeV/nucleon) using the Glauber model. The type of calculation used in those studies was the optical-limit and zero-range approximations of the Glauber theory, which is considered to be valid at high energies [2,3]. Later, these zero- or finite-range optical-limit Glauber-type calculations were used to extract the radial shapes of the nucleon density distributions from the energy dependencies of σ_R [4–6] or from the target dependence [7].

These studies indicate that at intermediate energies (several tens to several hundreds of MeV/nucleon) σ_R is highly sensitive to dilute density distribution such as a halo structure due to the large nucleon-nucleon total cross sections (σ_{NN}) at lower energies compared to those at higher energies. However, an insufficient understanding of $\sigma_R(E)$ at intermediate energies has impeded clear and precise discussions regarding the detailed radial distribution of dilute density at the nuclear surface.

There have been several attempts to study σ_R at intermediate energies within the framework of the Glauber model [8–13]. Unfortunately, in those studies, the level of agreement between the calculations and experimental results cannot be discussed within the uncertainty of ∼10%, owing to the lack of precise σ_R data. To study the nucleon density distributions from σ_R data using Glauber-type calculations in more detail, it is essential to obtain new and accurate data for $\sigma_R(E)$ at intermediate energies and to check the applicability of calculation more precisely.

For this reason, detailed investigations of σ_R were conducted for both stable and unstable nuclei, the densities of which have been well studied. We have precisely measured σ_R for ^{12}C using Be, C, and Al targets and have also measured σ_R for ^{11}Be, which is known to be a neutron-halo nucleus, on Be targets. The measurements were performed in the energy range of 30−400 MeV/nucleon where there is a lack of precise and systematic σ_R data, even for the stable nuclei. By testing several Glauber-type calculations with the present systematic σ_R data, a useful prescription was found that connects the appropriate nucleon density distributions with the σ_R at intermediate energies. In this Rapid Communication, we report on the good applicability of our method, which consists of a combination of the Fermi-motion effect and the Glauber model, by comparing the calculations with a number of σ_R data points for ^{12}C, ^{11}Be, and the proton-halo nucleus ^{8}B at intermediate energies.

All measurements were performed using the Heavy Ion Medical Accelerator in Chiba (HIMAC) synchrotron and the fragment-separator facility at NIRS (National Institute of Radiological Sciences, Japan) [14]. The σ_R for ^{12}C were measured using primary beams. For ^{11}Be, we used secondary beams produced through the projectile fragmentation of a 160 MeV/nucleon ^{13}C primary beam with Be production targets of different thicknesses. To perform measurements over a wide energy range, we adjusted the beam energies using

*takechi@ribf.riken.jp

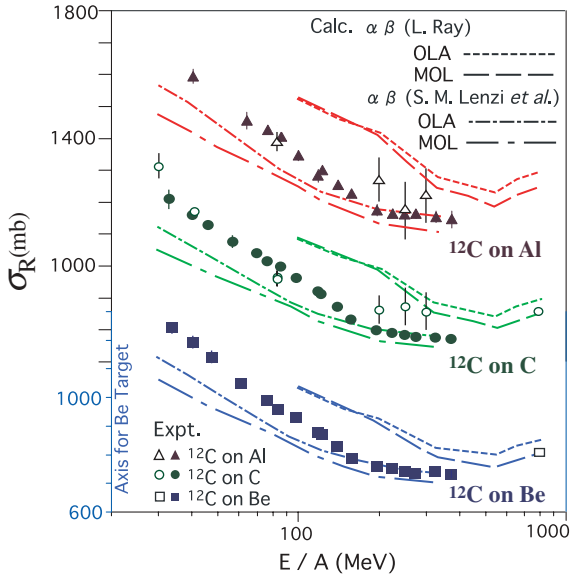

FIG. 1. (Color online) The σ_R data for ^{12}C as a function of beam energy. The closed symbols denote the present data and open symbols denote data from Refs. [8,25–27]. The OLA and MOL calculations were performed using the NN parameters from Ref. [22] (short and long dashed curves) and Ref. [23] (short and long dash-dotted curves).

energy degraders and the fragment separator at NIRS. The transmission method was employed to measure σ_R. Details regarding the experimental procedures are given in Ref. [15].

In Fig. 1, the experimental results of σ_R for ^{12}C obtained in the present study are indicated by closed symbols. In our experimental method, the main error in σ_R was due to contamination from inelastic-scattering events in the nonreacting events. The method used to estimate the number of these events are described in Ref. [5]. This method was modified through the use of Monte Carlo simulations [17] to make the estimations more realistic, and a good accuracy of 1–2% was achieved. Other existing data for stable nuclei are shown with open symbols for comparison. Existing data and the present data are consistent with one another within their experimental uncertainties.

We performed two types of calculations based on the Glauber theory to compare to the data. One is the optical-limit approximation (OLA) of the Glauber theory [18], which is used extensively in the analyses of σ_I at high energies. The other is the improved calculation formulated by B. Abu-Ibrahim and Y. Suzuki, which takes into account the higher-order multiple scattering effect than the OLA method does [19]. This method is referred to as the modified optical limit (MOL) calculation in this Rapid Communication. The following is a formulation of these two methods. In both the OLA and MOL calculations, σ_R is given by

$$\sigma_R = 2\pi \int b\, db[1 - e^{-2\mathrm{Im}\chi(\boldsymbol{b})}]C(E), \qquad (1)$$

where b is an impact parameter and $C(E)$ denotes the influence of the Coulomb force [4]. In the OLA calculation, $\chi(\boldsymbol{b})$ is expressed as

$$\chi(\boldsymbol{b}) = i \int ds \int dt \Gamma(\boldsymbol{b}+\boldsymbol{s}-\boldsymbol{t})\rho_z^P(\boldsymbol{s})\rho_z^T(\boldsymbol{t}),$$

TABLE I. Density parameters for stable nuclei used in the present work. The intrinsic quadrupole moment, Q_0, can be deduced from the observed quadrupole moment [16]. For ^{12}C, we derived Q_0 from $B(E2)$ value of the first excited state [16].

	rms radius (fm)	R_0	β_2	a	c	Q_0(mb)
^{9}Be	2.37	1.35	0.900	0.858	–	265
^{12}C	2.30	1.42	−0.623	1.906	–	198
^{27}Al	2.95	2.90	0.347	–	0.492	419

where Γ is the profile function, ρ_z^P, ρ_z^T are the z-integrated densities of the projectile and the target nuclei, respectively, and $\boldsymbol{s}$, $\boldsymbol{t}$ are the nucleon coordinates of the projectile and target in the plane perpendicular to the beam axis. In the MOL calculation, $\chi(\boldsymbol{b})$ is expressed as

$$\chi(\boldsymbol{b}) = \frac{i}{2}\int ds\ \rho_z^P(\boldsymbol{s})\left\{1 - \exp\left[-\int dt \rho_z^T(\boldsymbol{t})\Gamma(\boldsymbol{b}+\boldsymbol{s}-\boldsymbol{t})\right]\right\} + \frac{i}{2}\int dt\ \rho_z^T(\boldsymbol{t})\left\{1-\exp\left[-\int ds \rho_z^P(\boldsymbol{s})\Gamma(\boldsymbol{b}+\boldsymbol{t}-\boldsymbol{s})\right]\right\}$$

[19,20]. The profile function Γ is often parametrized as

$$\Gamma(\boldsymbol{b}) = \frac{1-i\alpha}{4\pi\beta}\sigma_{NN}(E)\exp\left(-\frac{\boldsymbol{b}^2}{2\beta}\right), \qquad (2)$$

where $\sigma_{NN}(E)$ is the nucleon-nucleon (NN) total cross section at kinetic energy E and β is the so-called finite-range parameter, which is related to the range of nuclear force. The parameter α is the ratio of the real and imaginary parts of the NN-scattering amplitude.

To perform the OLA and MOL calculations, we adopted proper projectile and target densities from experimental data. Nuclear densities of stable nuclei can be obtained by unfolding the experimental charge distribution [21] with the proton charge radius of 0.85 fm. Furthermore, the quadrupole deformations of the nuclei were taken into account as follows. The functional shape of the nuclear density is assumed to be of the harmonic-oscillator (HO) type [21] for ^{9}Be and ^{12}C, and of the Fermi type [21] for ^{27}Al, as represented by

$$\rho_{\mathrm{HO}}(r) = \int \rho_0 \left\{1 + a\left(\frac{r}{R(\theta)}\right)^2\right\}\exp\left[-\left(\frac{r}{R(\theta)}\right)^2\right]d\Omega,$$

$$\rho_{\mathrm{Fermi}}(r) = \int \rho_0 \Big/ \left(1+\exp\left[\frac{r-R(\theta)}{c}\right]\right).d\Omega,$$

where $R(\theta) = R_0[1 + \beta_2 Y_{20}(\theta)]$. The parameters β_2 and R_0 were determined through fits to the experimental intrinsic quadrupole moments and the root-mean-square charge radii. This deformation effect increases calculated σ_R values by 3% at most. The parameters a and c are fixed to the values obtained by unfolding the charge distributions. The parameter ρ_0 is determined by normalizing the integral of nucleon density to the mass number of the projectile or target nuclide. The parameters used in the calculations are given in Table I.

Using the densities mentioned above, we performed the finite-range OLA and MOL calculations. The parameters of the profile function [see Eq. (2)], α and β, were taken from

Refs. [22,23]. As for $\sigma_{NN}(E)$, the experimental NN total cross sections are available from Ref. [24]. In Fig. 1, the OLA and MOL curves calculated from the profile function parameters of Ref. [22] (short and long dashed curves) and Ref. [23] (short and long dash-dotted curves) are shown. Note that over almost the entire energy range, the OLA are larger in magnitude than those of the MOL calculations by several percent. When the calculations are compared to our new experimental data, it is clear now that there are some discrepancies between them. The Glauber-type calculations performed with the parameters from Ref. [22] overestimate σ_R by at least 10%. However, the calculations performed with the parameter set from Ref. [23] tend to underestimate σ_R, especially at energies below 200 MeV/nucleon. As can be seen from Fig. 1, the σ_R values calculated with these two parameter sets (dashed and dash-dotted curves) are quite different from one another. This observation was also pointed out by Horiuchi *et al.*, who performed almost the same calculations for the case of ^{12}C+^{12}C and compared them to our present data recently [28]. It is not clear what causes the differences between the data and calculations or between the two parameter sets of α and β. It thus appears that the existing parameter sets are rather ambiguous.

To study the nucleon density distributions of nuclei from $\sigma_R(E)$ at intermediate energies, it is desirable to find some prescription that can reproduce the experimental $\sigma_R(E)$ properly using the appropriate nucleon density distributions as inputs. For this purpose, we attempted to find a simple method to calculate σ_R using few number of free parameters on the basis of the MOL Glauber-type calculation. Here, we modify $\sigma_{NN}(E)$ used in the calculation, instead of adjusting the NN parameters α and β, by incorporating the Fermi motion of nucleons into $\sigma_{NN}(E)$. We first assume that the momentum distribution of nucleons in the nucleus follows a Gaussian shape according to the Goldhaber model [29]. The momentum distribution of a projectile nucleon relative to a target nucleon parallel to the beam axis ($p_{\rm rel}$) is expressed as,

$$D(p_{\rm rel}) = \frac{1}{\sqrt{2\pi(\langle p^2\rangle^P + \langle p^2\rangle^T)}} \times \exp[-(p_{\rm rel} - p_{\rm proj})^2/2(\langle p^2\rangle^P + \langle p^2\rangle^T)]. \quad (3)$$

Here, $\langle p^2\rangle^P$ and $\langle p^2\rangle^T$ denote the mean-square momenta of the projectile and target nucleon, respectively, and $p_{\rm proj}$ is the momentum of a nucleon with the same velocity as the projectile nucleus. For stable nuclei, the experimental value $\sqrt{\langle p^2\rangle} = 90$ MeV/c extracted from projectile-fragmentation data was used [29]. This seems to be reasonable because σ_R is governed by peripheral collisions where the projectile fragmentation process dominates. The momentum width is known to be narrow in the case of a halo nucleon. For ^{11}Be, the experimental value of $\sqrt{\langle p^2\rangle}$ =18.6 MeV/c [30] was adopted for the valence neutron, while 38.7 MeV/c [31] was used for the halo nucleon in ^{8}B. Using Eq. (3), the momentum-averaged total cross section of nucleons in the nucleus can be written as

$$\sigma_{NN}^{\rm eff} = \int_{-\infty}^{+\infty} dp_{\rm rel}\sigma_{NN}(p_{\rm rel})D(p_{\rm rel}). \quad (4)$$

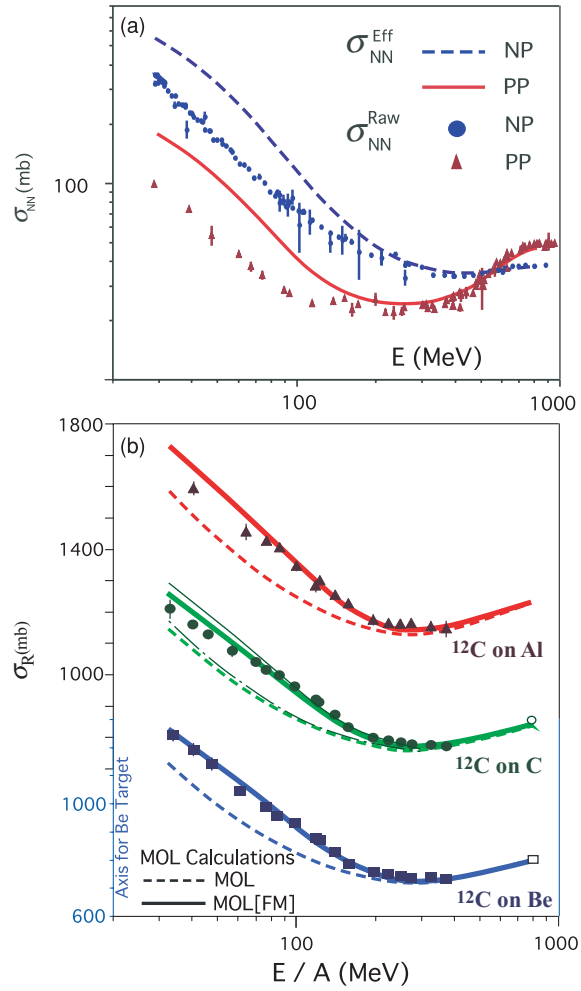

FIG. 2. (Color online) (a) Modified σ_{NN} as effective NN cross section ($\sigma_{NN}^{\rm eff}$), which is compared with the raw σ_{NN}. (b) MOL calculations with $\beta(E)$ from Eq. (4) (dashed curve) and MOL[FM] calculations (solid curve) are compared with experimental data. We also show the MOL and MOL[FM] calculations using a Gaussian-type density for the C target (thin solid and dot-dashed curves).

We describe this modified σ_{NN} as an effective NN cross section ($\sigma_{NN}^{\rm eff}$) that is compared with the raw σ_{NN} ($\sigma_{NN}^{\rm raw}$) in Fig. 2(a). The MOL calculations with $\sigma_{NN}^{\rm eff}$ (MOL[FM]) are indicated by solid curves in Fig. 2(b), which are seen to be in good agreement with the data. In the MOL[FM] calculation, we assume that the parameter α is equal to zero for simplicity. This assumption is often used when one discusses nucleus-nucleus reaction cross sections and does not intend to describe other exclusive physical quantities such as differential cross sections of elastic scattering [32]. Under this assumption, $\alpha = 0$, the β value can be uniquely determined as $\beta = \sigma_{NN}^{\rm tot}/16\pi$ below 300 MeV/nucleon, as discussed in Refs. [19,28]. At higher energies we used $\beta = 0.14$ fm^2, which represents an average of the high-energy β values given in Refs. [22,23]. We do not take a momentum average of β, because its energy dependence is rather moderate and would only change the calculations by about 2% at most. The

deviation of the σ_R data from the MOL[FM] calculations is evaluated by a reduced χ^2 value of 2.4, which indicates a reasonable fit. Although we do not completely understand the physical propriety of our method, it is very interesting that the energy dependences of σ_R are so naturally reproduced as seen in Fig. 2(b). In addition, MOL calculations were performed without Fermi-motion effect using the same α, β and experimental $\sigma_{NN}(E)$. The results of calculations are indicated by dashed curves in Fig. 2(b). Those values are found to be 5–10% smaller than those of the MOL[FM] calculations below 200 MeV/nucleon. We also show MOL[FM] and MOL calculations for the C target using a Gaussian-type nuclear density distribution, the rms radius of which is the same as that used for the HO type (thin solid and dot-dashed curves). The results of the calculations are only slightly different in the lower energy region due to differences in the functional shapes of two densities, however, it can be seen that the MOL[FM] calculations are satisfactory in both cases.

In these calculations we did not take into account the Pauli-blocking effect. It was indicated in Refs. [9,33] that the Pauli-blocking and Fermi-motion effects are very small at high energies where the relative momentum between two colliding nucleons is large compared to the Fermi momentum. At lower energies, on the other hand, it was indicated that the strong Pauli-blocking effect is dominant over the Fermi-motion effect, which reduces σ_R considerably. However, a recent study [34] pointed out that the reduction effect on σ_R is much smaller due to the fact that the reaction probability is governed by nucleon scattering at the peripheral part where the nucleon density is relatively low. In the present work, we did not take into account such reduction effects caused by Pauli blocking; instead, we take into account the increasing effect of the Fermi motion using the momentum distribution of projectile fragments that were determined experimentally.

It should be noted that the methods used to incorporate the Fermi-motion effect and NN parameters may be too simple to discuss the absolute magnitude of the Fermi-motion effect. It is nonetheless interesting to note that energy dependences of σ_R fit the data very naturally following the inclusion of the Fermi-motion effect.

The discussions above are restricted to the stable nuclides. To test whether this method is applicable to unstable nuclei, the two halo nuclides ^{11}Be and ^{8}B were studied. These were chosen because their structures and density distributions are relatively well known. In Fig. 3, we show the σ_R data for ^{11}Be on Be. The closed symbols are data from the present study and open symbols represent data taken from Refs. [4,35]. These data sets are compared to two types of Glauber calculations; the MOL calculations with $\sigma_{NN}^{\rm eff}$ (MOL[FM]; solid curve) and σ_{NN} (MOL; dashed curve). In these MOL calculations the same values of α and β were used as for the stable nuclei. For the nucleon density distribution of ^{11}Be, the shell-model density from Ref. [37] was adopted. The spectroscopic factor for the $2s_{1/2}$ configuration for the valence neutron resulting from this calculation is in very good agreement with the value deduced in a recent Coulomb-breakup experiment [38].

Figure 3 indicates that the same tendencies exist between the experimental data and the calculations as for the stable nuclei. The MOL[FM] calculations (solid curve) seem to

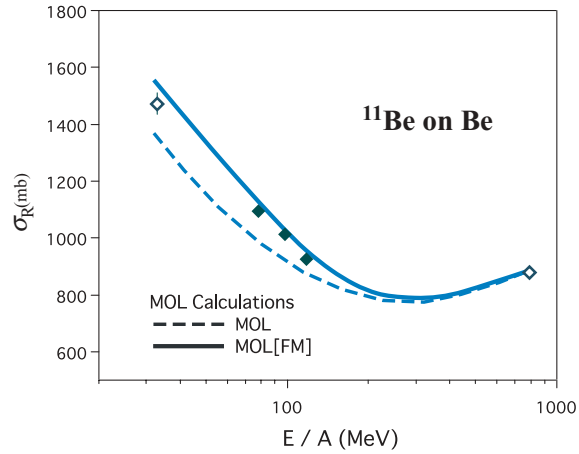

FIG. 3. (Color online) The σ_R data for ^{11}Be compared with MOL (dashed curve) and MOL[FM] (solid curve) calculations. The closed symbols are present data and open symbols are from Ref. [4].

reproduce σ_R reasonably. To perform the MOL[FM] calculations, it was assumed that $\sqrt{\langle p^2 \rangle} = 90$ MeV/c for the core and 18.6 MeV/c for the halo neutron to account for its narrow momentum width. This effect reduces σ_R slightly at energies around 30 MeV/nucleon (about 1–2%) but becomes negligible at energies higher than 50 MeV/nucleon.

We also compared the MOL[FM] calculations with σ_R data for ^{8}B. The data for ^{8}B were taken from Refs. [5,35,36,39]. In the calculations, the multicluster-model density for ^{8}B [40] was used, which can reproduce the experimental quadrupole moment of ^{8}B quite well [41]. We used a value of 90 MeV/c for $\sqrt{\langle p^2 \rangle}$ in the core and 38.7 MeV/c [31] for the valence part. The value of the NN parameters α and β were the same

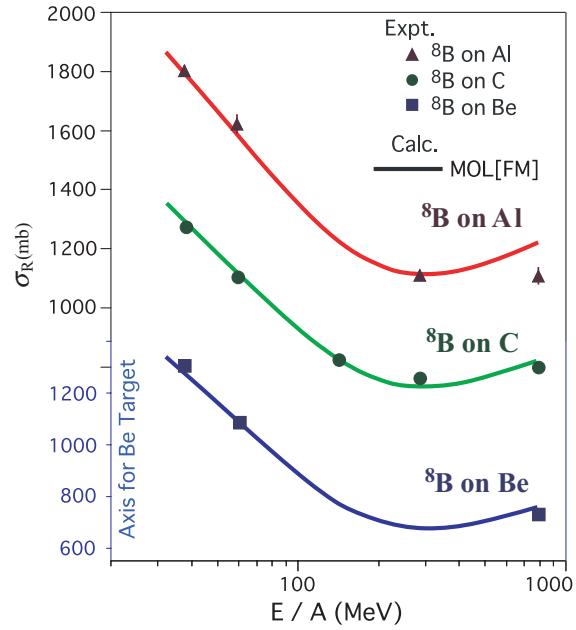

FIG. 4. (Color online) The σ_R data for ^{8}B compared with MOL[FM] (solid curve). The data for ^{8}B were taken from Refs. [5,35,36].

as those used in the previous calculations. From Fig. 4, it can be seen that the MOL[FM] calculations reproduce the data satisfactory, albeit with the exception of the data point at 790 MeV/nucleon from the Al target.

In the MOL[FM] calculations introduced in this Rapid Communication we did not adjust any parameters to fit the data from different nuclides. Just the same α and β parameters, experimentally determined momentum distributions and appropriate experimentally supported nucleon density distributions were used. It is interesting that σ_R for various different nuclei, even the halo nuclei, are reproduced successfully without any adjustment of the parameters.

In summary, we made precise measurements of σ_R for ^{12}C and the neutron-halo nucleus ^{11}Be on light-mass targets at intermediate energies. The energy dependencies of σ_R over a wide energy range were obtained and it is now possible to discuss the agreement between experimental σ_R data and calculations more precisely than before. We found that by combining the Fermi-motion effect and the finite-range MOL Glauber-type calculation, the energy dependencies of σ_R can be reproduced nicely over a large energy range when using appropriate nucleon-density distributions as inputs. We compared the results of the calculations to our data and other existing data and showed that our method can be applied to various nuclei, including exotic halo nuclei. Although further study on the propriety of our method is desirable, it currently provides a useful prescription with which to study the radial shapes of nucleon-density distributions from σ_R and to investigate the nuclear surface structure.

We thank Yasuyuki Suzuki and Akihisa Kohama for their helpful discussions. This work was supported by Research Project with Heavy Ions at NIRS-HIMAC and was partially funded by the Sasakawa Scientific Research Grant from The Japan Science Society, and also by the Grant-in-Aid for Scientific Research (C) from Japan Society for the Promotion of Science.

[1] I. Tanihata, J. Phys. G **22**, 157 (1996), and references therein.
[2] R. Glauber, in *Lectures in Theoretical Physics*, edited by W. Brittin and L. Dunham (Inter science, New York, 1959).
[3] P. J. Karol, Phys. Rev. C **11**, 1203 (1975).
[4] M. Fukuda *et al.*, Phys. Lett. **B268**, 339 (1991).
[5] M. Fukuda *et al.*, Nucl. Phys. **A656**, 209 (1999).
[6] Y. Yamaguchi *et al.*, Phys. Rev. C **70**, 054320 (2004).
[7] I. Tanihata *et al.*, Phys. Lett. **B287**, 307 (1992).
[8] S. Kox *et al.*, Phys. Rev. C **35**, 1678 (1987).
[9] M. S. Hussein, R. A. Rego, and C. A. Bertulani, Phys. Rep. **201**, 279 (1991).
[10] Y. G. Ma, W. Q. Shen, J. Feng, and Y. Q. Ma, Phys. Rev. C **48**, 850 (1993).
[11] C. Xiangzhou *et al.*, Phys. Rev. C **58**, 572 (1998).
[12] M. Ismail, A. Y. Ellithi, and H. Abou-Shady, Phys. Rev. C **71**, 027601 (2005).
[13] A. Bhagwat and Y. K. Gambhir, Phys. Rev. C **73**, 024604 (2006).
[14] M. Kanazawa *et al.*, Nucl. Phys. **A746**, 393 (2004).
[15] M. Takechi *et al.*, Eur. Phys. J. A **25**, 217 (2005).
[16] R. B. Firestone, *Table of Isotopes*, 8th ed. (John Wiley & Sons, Inc., New York, 1996).
[17] M. Takechi, Ph.D. thesis, Osaka University, 2006.
[18] P. Karol, Phys. Rev. C **46**, 1988 (1992).
[19] Y. Suzuki, R. Lovas, K. Yabana, and K. Varga, *Structure and Reactions of Light Exotic Nuclei* (Taylor & Francis, London, 2003).
[20] B. Abu-Ibrahim and Y. Suzuki, Phys. Rev. C **62**, 034608 (2000).
[21] H. DeVries, C. W. DeJager, and C. DeVries, At. Data Nucl. Data Tables **36**, 495 (1987).
[22] L. Ray, Phys. Rev. C **20**, 1857 (1979).
[23] S. M. Lenzi, A. Vitturi, and F. Zardi, Phys. Rev. C **40**, 2114 (1989).
[24] P. D. Group, Eur. Phys. J. C **3**, 1 (1998).
[25] C. Perrin *et al.*, Phys. Rev. Lett. **49**, 1905 (1982).
[26] D. Q. Fang *et al.*, Phys. Rev. C **61**, 064311 (2000).
[27] A. Ozawa *et al.*, Nucl. Phys. **A693**, 32 (2001).
[28] W. Horiuchi, Y. Suzuki, B. Abu-Iburahim, and A. Kohama, Phys. Rev. C **75**, 044607 (2007).
[29] A. S. Goldhaber, Phys. Lett. **B53**, 306 (1974).
[30] J. H. Kelley *et al.*, Phys. Rev. Lett. **74**, 30 (1995).
[31] M. H. Smedberg *et al.*, Phys. Lett. **B452**, 1 (1999).
[32] R. E. Warner, Phys. Rev. C **74**, 014605 (2006).
[33] N. J. DiGiacomo *et al.*, Phys. Rev. Lett. **45**, 527 (1980).
[34] R. E. Warner, Phys. Rev. C **65**, 044617 (2002).
[35] I. Tanihata *et al.*, Phys. Lett. **B206**, 592 (1988).
[36] B. Blank *et al.*, Nucl. Phys. **A624**, 242 (1997).
[37] H. Sagawa, Phys. Lett. **B286**, 7 (1992).
[38] N. Fukuda *et al.*, Phys. Rev. C **70**, 054606 (2004).
[39] K. Obuchi *et al.*, Nucl. Phys. **A609**, 74 (1996).
[40] K. Varga, Y. Suzuki, and I. Tanihata, Phys. Rev. C **52**, 3013 (1995).
[41] T. Sumikama *et al.*, Phys. Rev. C **74**, 024327 (2006).